The Advanced Ducted Propulsor in the Upgraded 9- by 15-Foot Low Speed Wind Tunnel

David B. Stephens[1] and David M. Elliott[1]
NASA Glenn Research Center, Cleveland, OH, 44135, USA

John A. Gazzaniga[2]
HX5, LLC, Fort Walton Beach, Florida, 32548, USA

A low pressure ratio, variable pitch scale model of an aircraft engine fan was tested in the NASA Glenn Research Center 9- by 15-Foot Low Speed Wind Tunnel. The Advanced Ducted Propulsor designed by Pratt & Whitney in the 1990's and has been part of multiple wind tunnel test campaigns over the intervening years. The most recent test served to commission the wind tunnel after an improvement project that lowered the background noise in the facility. A side benefit of the commissioning test was to generate new aerodynamic and acoustic measurements of this propulsor with the latest data systems and processing. The results of the test are reported as an open and non-proprietary data set for the aeroacoustics and propulsion community. New capabilities of the facility are also highlighted.

I. Nomenclature

M_0	=	tunnel freestream Mach number
RPMc	=	RPM corrected to standard day temperature, $\frac{RPM}{\sqrt{\Theta}}$
p_f^2	=	mean square sound pressure measured from an engine with forward flight
p_s^2	=	mean square sound pressure measured from a static engine test
α	=	convective amplification constant due to forward flight
Θ	=	total temperature of the air in the wind tunnel divided by the standard day temperature
θ_e	=	emission angle between source and receiver
θ_g	=	geometric angle between source and receiver

II. Introduction

An extensive upgrade to the 9- by 15-Foot Low Speed Wind Tunnel (9×15 LSWT) at NASA Glenn Research Center (GRC) was conducted between 2016 and 2019. A series of reports on the project were presented at the AIAA Aviation 2021 Forum [1] [2] [3] [4] with additional details documented in recent NASA Technical Memorandums [5] [6]. The primary purpose of the upgrade was to reduce the background noise in the test section to improve signal-to-noise ratio of microphone measurements. Acoustic measurements in the 9×15 LSWT are typically acquired using in-flow microphones, so the sensors are exposed to any unwanted noise present in the test section, whether generated in the test section or elsewhere in the tunnel loop. A secondary objective of the upgrade was to improve the anechoic quality of the test section to give more confidence that the measured sound was directly from the model being tested and not reverberating from the test section walls. These improvements were verified at the end of the improvement project, but only for an empty test section.

---

[1] Research Engineer, Acoustics Branch, AIAA Lifetime Member.
[2] Research Engineer, Acoustics Branch

During the period where the tunnel was under construction and there was no testing, the mechanical, hydraulic, pneumatic, control and data systems required for testing scale model aircraft propulsor fans were completely removed and replaced. Much of the original equipment had been accumulated and developed over decades of fan testing, so this was an opportunity to revisit and update the hardware, electronics, cables and tubing. There was a consensus that implementing a vast amount of new equipment simultaneously would result in some risk when operating a fan model. Instead of testing a new fan model with an external partner, the choice was made to conduct a commissioning test using an existing, previously tested NASA-owned fan model to demonstrate safe operation and accurate data collection. The present report is a summary of that commissioning test.

This report is a companion piece to a NASA Technical Memorandum [7] which is a test report including supplemental files of data and geometry. The following sections give a brief history on testing aircraft propulsors in the 9×15 LSWT, then a short description of the commissioning test and finally some observations from the data.

III. Propulsor Testing in the 9×15 LSWT

The 9×15 LSWT was built in the return leg of the 8- by 6-foot Supersonic Wind Tunnel (8×6 SWT) in 1969. Built for testing the aerodynamic performance of short and vertical lift propulsion concepts, it had 0.5 inch (12 mm) aluminum plate making up the walls, floor and ceiling [8]. As interest in studying aircraft engine noise grew, 2 inch (5 mm) thick fiberglass panels were added to provide sound dampening, with the depth of the panels subtracting from the cross sectional area. The acoustic quality of the test section was documented in 1976 by Rentz [9]. A focus on propeller noise motivated the design and implementation of a 13 inch (34 cm) deep variable density liner [10], which was installed in 1986. This deep liner was fit between the steel beam structure of the test section frame, while a shallow 2 inch (5 cm) liner was maintained over the beams. The flow surface was a perforated steel plate. The no-flow acoustic quality of this test section was documented in the early 1990’s by Dahl and Woodward [11] [12]. The background noise of the tunnel as measured in the test section was reported in 1995 by Woodward et al. [13], specifically focusing on new streamlined microphone holders. The new microphone holders successfully reduced the self-noise of the microphone system to a level such that the tunnel self-noise was now dominant for empty tunnel measurements. It was known for years that the tunnel needed to be operated at Mach 0.1 to limit background noise levels when testing quiet models or at low fan speeds, but as reported in Figure 7 of [13], flow speeds of Mach 0.05 were found to be sufficient to provide inflow turbulence clean-up. The acoustic environment of the 9×15 LSWT was essentially unchanged for the next 20 years [14].

A. Background vs Propulsor Noise

The NASA / Pratt & Whitney Advanced Ducted Propulsor (ADP) Fan 1 was used during a test campaign of aircraft engine liners during 1996 and 1997, pictured in Figure 1. The details of the fan model will be discussed more in Section IV A, but in short, the fan was expected to be very quiet. Microphone measurements were made using a traversing microphone on a track, along with a few fixed microphones. To limit the tunnel background noise level, most testing was conducted at Mach 0.1. An example sound measurement made with the traversing microphone broadside to the ADP fan model at a corrected speed of 4950 RPMc is shown in Figure 2. Also shown in the graph are empty tunnel measurements at Mach 0.1 and Mach 0.2. There is 10+ dB of signal above the Mach 0.1 empty tunnel background noise at most frequencies while at Mach 0.2 the empty tunnel noise would be louder than the fan noise. The bulk of the data for this fan test was acquired at Mach 0.1, although high power conditions were measured at Mach 0.2 with good signal above the background level.

Figure 1 - ADP fan test in 1996

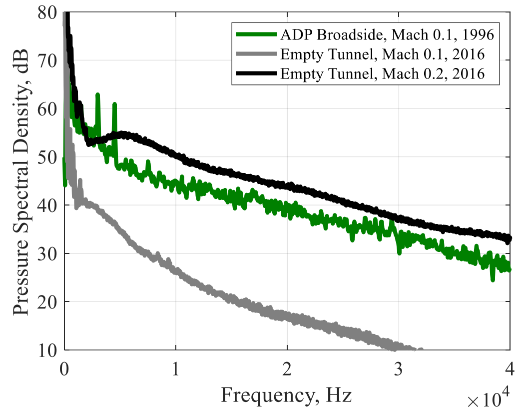

Figure 2 - ADP fan noise compared with legacy tunnel background levels

In contrast to fan models, propellers have typically been tested at tunnel speeds of Mach 0.2. This is because there is no duct to clean up the inflow to the rotor so data collection must take place at representative forward flight speeds. The sensitivity to the tunnel Mach number was investigated by taking measurements at Mach 0.18 and Mach 0.22 along with Mach 0.20, as shown given in Tables 5 and 7 of [15]. Mach 0.22 is the reliable upper limit of the 9×15 LSWT operating envelope. The open rotor test is pictured in Figure 3. An example sideline spectra measurement with the rotor at 4628 RPMc is given in Figure 4. Tones are easily identifiable in the measurement while the broadband noise has minimal signal above the background noise.

Figure 3 – Open rotor propulsion rig 2010 test

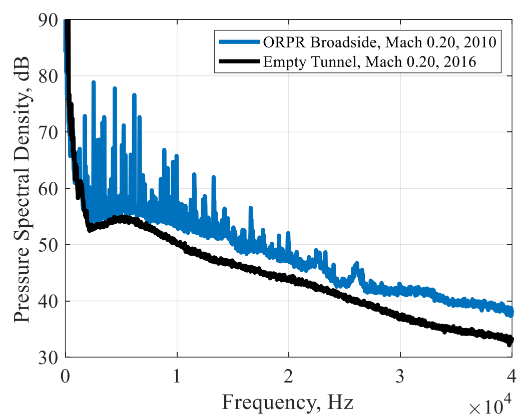

Figure 4 - Acoustic data from ORPR 2010 test along with appropriate empty tunnel measurement

B. Wind Tunnel Acoustic Upgrade

Motivated by these issues and in anticipation of future propulsors that are either quieter, require a realistic forward flight velocity or both, a tunnel renovation was advocated for by NASA researchers and industry partners. The successful outcome was reported on in references [1] to [6] as previously cited, but will be very briefly summarized here for convenience. The empty tunnel background noise reduction is shown in Figure 5, both before and after the upgrade. The reduction in background noise was around 10 dB for a wide range of frequencies. More detailed observations are given in Figure 21 of [6] and supporting text. The acoustic quality before and after the renovation was quantified by three different methods, described in Sections 5 through 7 of [6]. A snapshot of the results is given in Figure 6, which presents the result from a draw-away test. For this test, a point source speaker emits a tone and a microphone is drawn away. Standing waves in the room cause constructive and destructive interference. The microphone quantifies this as a fluctuation in the tone level. This is repeated for different frequencies and source/receiver layouts. In summary, the reduction in uncertainty was reduced about 2.5 dB above 500 Hz, as quantified by this metric.

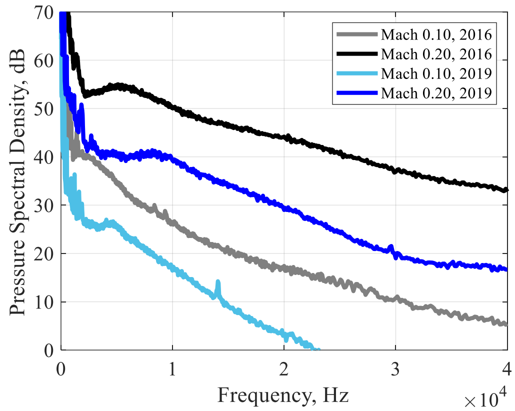

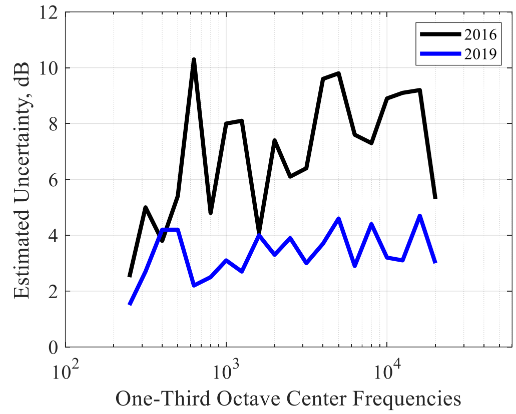

Figure 5 - Empty tunnel noise before and after upgrade

Figure 6 - Sample anechoic quality before and after upgrade

IV.Commissioning Test

Along with the upgraded test section and other acoustic treatments, the opportunity of a multi-year shutdown enabled other systems to be replaced and upgraded. The 8×/9× wind tunnel complex is one of the busiest wind tunnels at NASA and major system upgrades had previously been delayed if they might cause the facility to be unavailable for months at a time. Empty tunnel measurements were made with the new traversing microphone system in late February 2020, and then testing was stopped due to the global pandemic. Before the 9×15 LSWT commissioning test could resume, however, several high-priority tests took place in the 8×6 SWT. Tunnel occupancy for the ADP test began on 17 February 2022, the first checkout run began on 27 May 2022, the first research run was 13 June 2022 and the fan model was removed on 29 June 2022.

The fan test was completed successfully, demonstrating both the re-implementation of the ultra-high bypass drive rig capability and the safe operation of the tunnel and fan model. Aerodynamic and acoustic data compared favorably to a prior test with the same model [7]. The commissioning test also served as a risk-reduction procedure for a larger and more complicated fan test that was successfully conducted in 2024-2025. The rest of this section is a short summary of the test and a discussion of the resulting data.

A. Advanced Ducted Propulsor Fan 1

The 22-inch (56 cm) diameter Advanced Ducted Propulsor Fan 1 was designed by Pratt & Whitney in the early 1990’s. It was designed as a high-bypass ratio, low-tip speed, low-pressure ratio turbofan model with variable pitch fan blades, reconfigurable for a variety of wind tunnel testing applications. Specifically at cruise, the design bypass ratio is 13.3, the fan tip speed is 806 ft/s (246 m/s) and the pressure ratio is 1.29. It is a 5.91 scale model for a concept 130 inch (330 cm) diameter engine making 60,000 lbf (267 kN) of thrust. An extensive contractor report was delivered to NASA along with the fan model and describes the aerodynamic, structural and acoustic design [16]. Reports from previous tests have been published on performance [17], acoustics [18] and noise predictions [19], among others. The model is equipped for testing acoustic liners, with inlet, interstage and aft liner bays. The present test utilized the hardwall configuration. The fan blades were set to the take-off pitch angle of -9°. The model has a passive core without a rotating booster. The core exhausts into the wind tunnel downstream of the bypass exhaust. The ADP flow paths are shown in Figure 7.

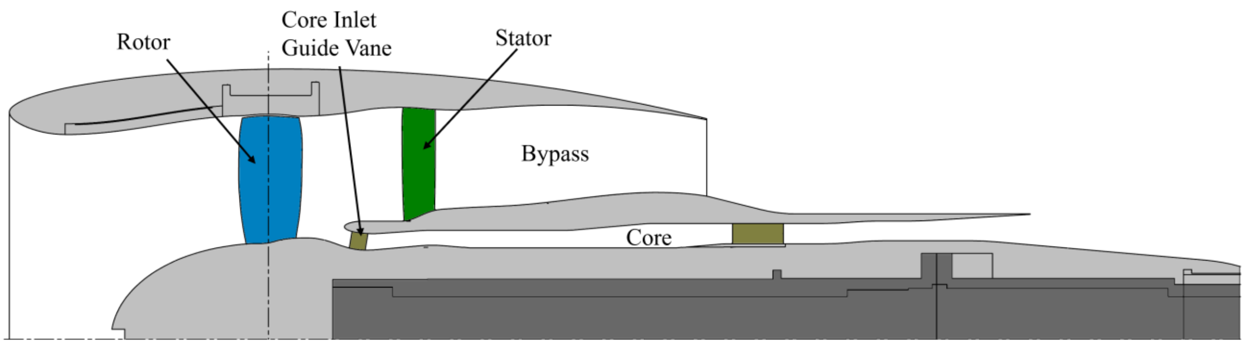

Figure 7 - Line drawing of ADP 22 inch fan model

The fan model is assembled on the NASA Ultra High Bypass (UHB) drive rig [20], a four stage turbine driven by heated compressed air. The fan model can be used with an inlet bellmouth and variable fan exit nozzle to allow fan mapping while testing in the wind tunnel, allowing relatively quick change between aerodynamic and acoustic configurations. For the present test, only the flight inlet and nozzle were used and no fan mapping was conducted. The UHB rig is mounted on a turntable on the floor of the 9×15 LSWT so the model can be turned in the horizontal plane to represent an inflow angle-of-attack, although this was not used in the present test. The fan model in the renovated test section is shown in Figure 8.

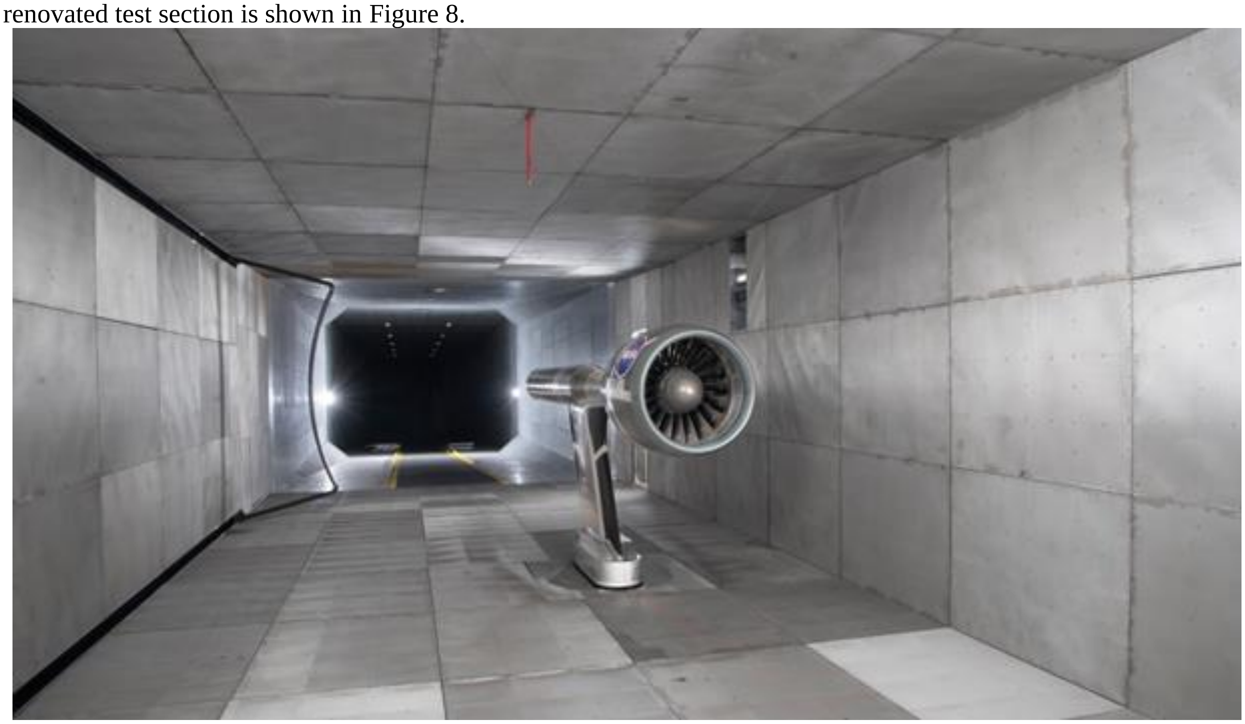

Figure 8 - NASA / P&W Advanced Ducted Propulsor in the 9×15 LSWT in 2022, acoustic configuration

B. Aerodynamic Measurements

Extensive pressure and temperature instrumentation is embedded throughout the fan model. Some sensors are integral and flush mounted with the flow surfaces, while others are part of rakes that span the flow passage. External measurements are also used, including an upstream flow rake to measure the streamtube ingested into the fan. The instrumentation is thoroughly described in Figures 3 through 5 of reference [17]. Other diagrams, photographs and illustrations are in the test summary report for the commissioning test [7]. The principal instrumentation for measuring fan aerodynamic performance are the Station 12.5 rakes, which are installed between the rotor and stator and span the bypass flow path. The assembled fan model is pictured in Figure 9.

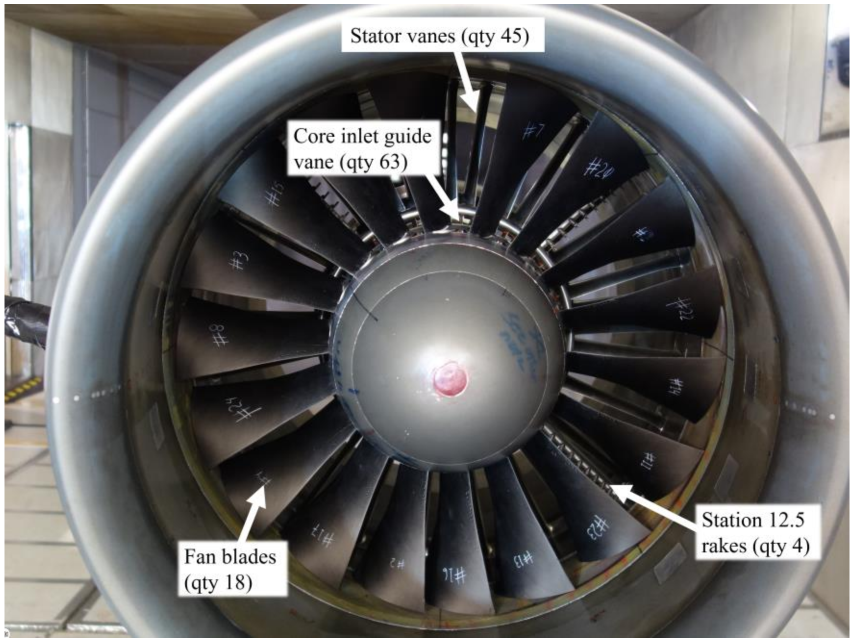

Figure 9 – Assembled fan model, front view

Temperature and pressures measured throughout the fan model are used to calculate temperature and pressure ratios along with mass flows, giving the major performance parameters for the fan model.

C. Acoustic Measurements

A new traversing microphone system was developed, with drive belt and motor systems in the upper and lower corners of the south wall of the wind tunnel, visible at left side of Figure 8. This is essentially outside the acoustic environment since the area was empty space between the acoustic boxes and the new external tunnel steel frame. The curved shape traces out a section of a cylinder with axis coincidence with the fan model. Five microphones are installed on the carbon fiber composite armature. The microphones are numbered 1 to 5 from top to bottom. The middle microphone is aligned with the midplane of the test section, matching the fan model. The other microphones are ±15° and ±25° azimuthally from the center of the fan model.

The inflow microphones are installed using aerodynamic fairings that extend upstream from the strut such that the microphone diaphram is 12 inches (305 mm) from the strut airfoil leading edge. The microphones are each equipped with a Flow Induced Tone Eliminator (FITE) Aerodynamic Microphone Forebody (AMF) and associated windscreen as designed at NASA Ames Research Center in the 1990's [21] [22]. Acoustic methods used in the 9×15 LSWT are described by the NASA Technical Memorandum of the same name [23].

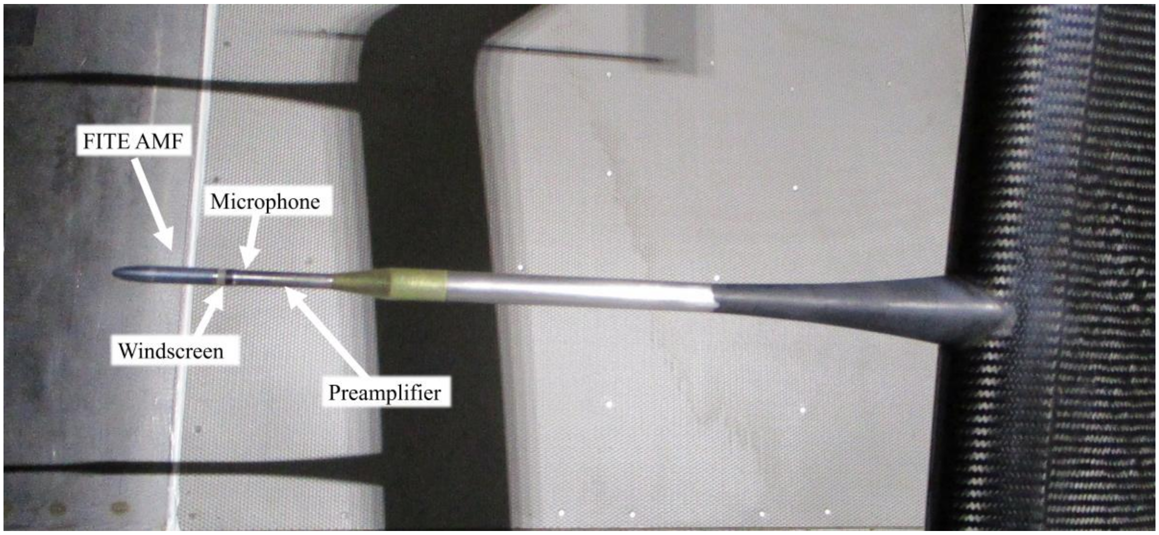

Figure 10 - Close view of microphone instrumentation

V.Implications for Propulsor Testing

The successful tunnel improvement project has several implications for propulsor testing, which will be discussed in this section. The capabilities that will be discussed include:

A. The effect of tunnel Mach number on a propulsor can be investigated in detail. The lower background noise of the 9×15 LSWT allows a full acoustic test matrix of fan speed and tunnel speed combinations to be acquired, while previously testing at high tunnel speeds was only possible with high fan speeds due to background noise.
B. Relatedly, this opens new testing capabilities. Quiet propulsors that would have been below the tunnel background noise level can now be measured. This also enables testing of propulsors that require a realistic forward flight speed can be conducted, such as propellers or ducted fans with very short inlets.
C. Mach 0.1 in the 9×15 LSWT is typically close to 113 ft/s (34 m/s) or 124 km/h, which is about half of the takeoff speed of a typical commercial aircraft. Testing at Mach 0.2 is on target for obtaining acoustic data with the airflow speed for the necessary rating conditions.
D. Details of forward flight effect on fan noise for system studies can be better investigated.

A. Effect of Tunnel Mach

1. On Fan Aerodynamics

The fan model was operated over a range of 12 speeds from 3500 to 9480 RPMc and with four tunnel speeds of Mach 0.1 to Mach 0.22, making for 48 test conditions. There was one model change, from an aerodynamic to acoustic configuration and the same 48 test points were repeated. The aerodynamic configuration includes the Station 12.5 rakes and an associated external instrument tube. These are removed for the acoustic configuration, shown in Figure 8. Specific shaft speeds of interest include approach, cutback and takeoff at 5425, 7525 and 8750 RPMc, respectively.

The four Station 12.5 rakes each have 10 temperature and pressure sensing elements. Momentum averaged pressure and temperature ratios are shown for the takeoff fan speed and four tunnel Mach numbers in Figure 11, along with resulting efficiency. It appears that increasing forward flight speed unloads the fan tips more than the hub, causing a drop in efficiency as measured at the outer part of the bypass flow path. This trend is not consistent across fan speeds however. As shown in Figure 12, for low fan speeds increasing tunnel Mach number increases efficiency. It is evident that on average, for a given fan speed, increasing the axial Mach number would decrease the angle of attack on the blades. At 8750 RPMc, as given in Figure 12, this causes a decrease in efficiency of about 1.5%. At speeds below about 8000 RPMc, and especially for values around the approach speed of 5425 RPMc, the efficiency increases with tunnel speed, also by about 1.5%. This suggests that external flight speed does have a significant effect on the fan aerodynamics, even with a relatively long inlet (L/D = 0.58) as this model has.

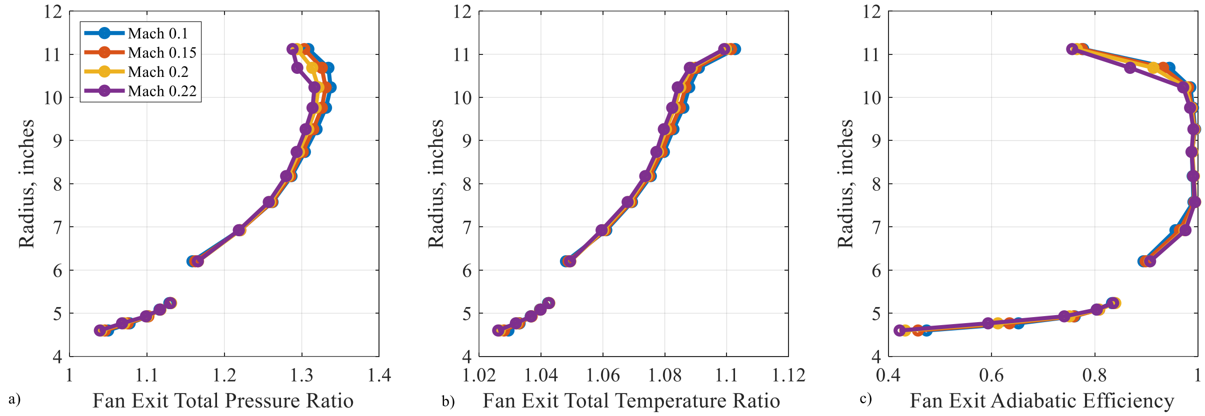

Figure 11 - Fan exit measurements at 8750 RPMc

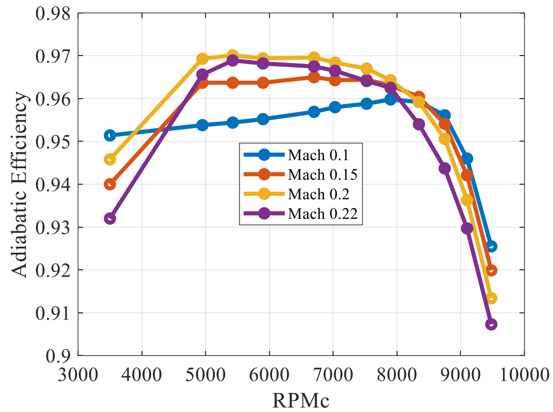

Figure 12 - Momentum averaged fan adiabatic efficiency at various forward flight speeds

Another significant effect of the flight speed on the aerodynamics was in the bypass ratio. At high fan speeds, the mass flow through the bypass is relatively insensitive to the external flight speed, as seen on the right side of Figure 13. In contrast, the core mass flow increases significantly even for high fan speed, as shown in Figure 14. A possible explanation is that increasing the tunnel free stream lowers the exit static pressure of the core flow more than the bypass flow, pulling more air through the core. The result is that the bypass ratio decreases significantly with increasing tunnel speed, plotted in Figure 15. Depending on the sensitivity of the fan model to the flow distribution and implications for testing an isolated engine component, it might be worthwhile to include a core weight flow control device. This model has provisions for core suction, but it was not used for the present test. To the authors knowledge, this capability has never been exercised with this fan model.

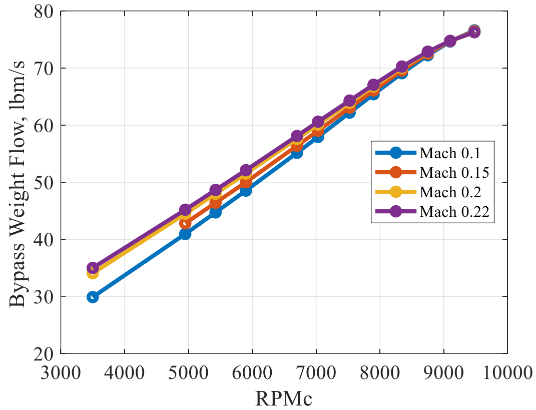

Figure 13 - Bypass flow rate

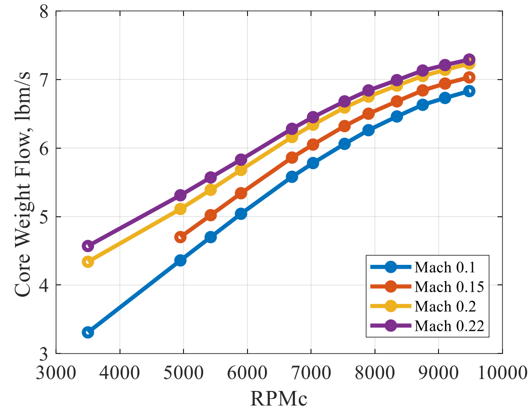

Figure 14 - Core flow rate

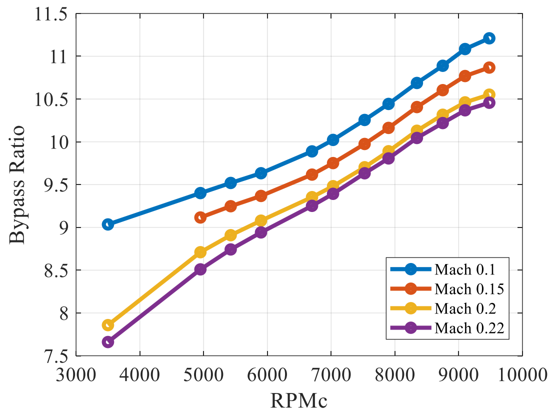

Figure 15 - Bypass ratio

2. On Fan Noise

The full matrix of fan speed and tunnel speed combinations allows some trends to be identified about fan noise, at least for the present model. A thorough assessment is beyond the scope of the present paper, but a few observations will be made. First, since the microphone recordings were made using a traversing sideline with the probe continually moving, it needs to be broken up into small segments. The tone/broadband separation algorithm developed by Sree and Stephens [24] was used to calculate tone and broadband spectra from each time series. A digital high-pass filter at 800 Hz was used to remove the lowest frequency part of the spectrum which makes the separation algorithm more reliable. For single shaft rotating systems, a phase averaging approach would normally be sufficient but since the microphone is in continuous motion the signals not perfectly periodic, which is the exact situation the algorithm was developed to address. Since the precise microphone location is known during the measurement, a de-dopplerization procedure could probably be developed as an alternative. An example result is shown in Figure 16. Since the sound convects in the tunnel with the flow speed, the sound directivity is plotted with respect to the emission angle, θ_e, which is calculated from the geometric angle, θ_g, and the tunnel Mach number, M_0, as, $\theta_e = \theta_g - \arcsin(M_0 \sin(\theta_e))$. See Figure 10 of [23] for more details.

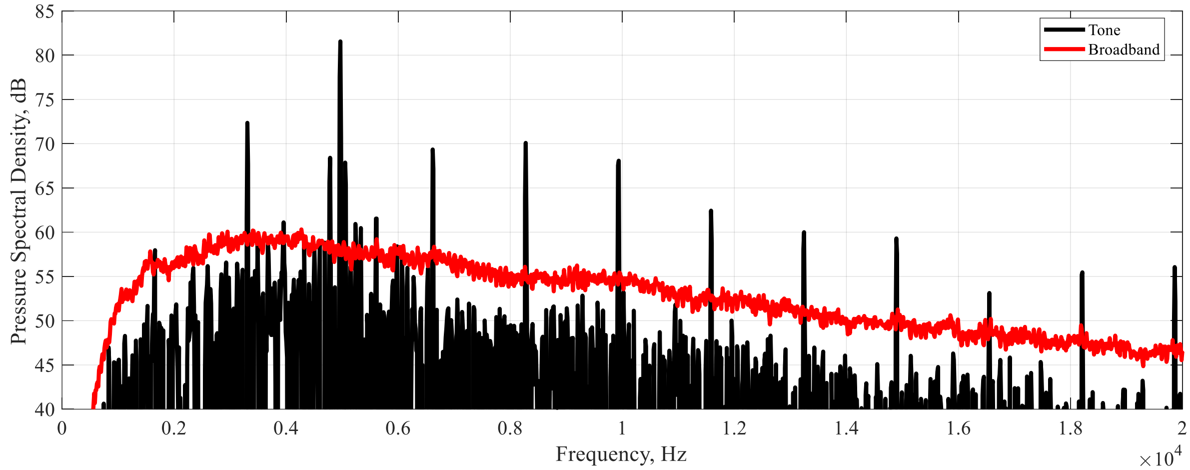

Figure 16 - Example tone and broadband sound spectra at 5425 RPMc and Mach 0.1, emission angle 40°

With the tone and broadband separated, a few trends could be quantified as a function of tunnel speed. The broadband sound spectral density was integrated over all frequencies to give a broadband OASPL, shown in Figure 17 for approach shaft speed and in Figure 18 for the takeoff shaft speed. Note the different y-axis limits. The shape of the directivity and the changes with tunnel speed are quite different at the two different rotor settings. At approach, increasing the tunnel Mach from 0.1 to 0.15 decreases forward broadband noise by around 0.5 dB and aft broadband noise by about 1 dB. Further increases to Mach 0.2 and 0.22 have a small effect, although details of the effect of the minimum around 70 degrees emission angle are still being investigated. At takeoff fan speed, the forward sound is decreased by about 1.5 dB between Mach 0.1 and 0.2 for emission angles around 50 degrees. At other angles, the effect of tunnel Mach is minimal. Presumably this is because the aft-dominant nature of the broadband noise at high fan speeds is largely insensitive to inflow conditions.

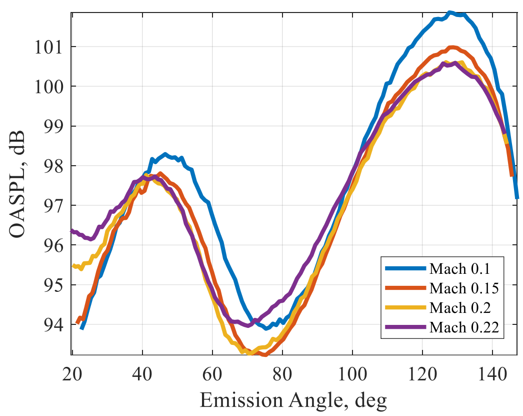

Figure 17 - Broadband sound level at 5425 RPMc

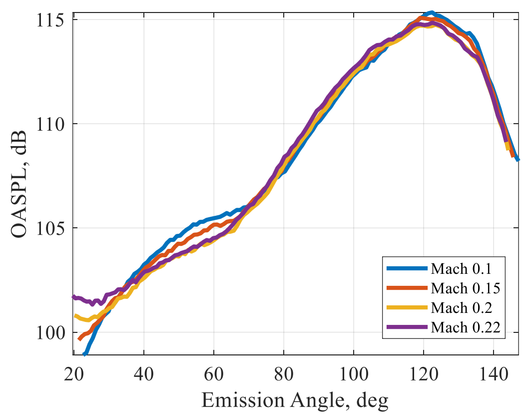

Figure 18 - Broadband sound level at 8750 RPMc

The findings for tones is naturally more complicated, as the tones can constructively and destructively interfere and are thus sensitive to myriad small details. The first blade passing tone (shaft rate multiplied by number of blades) generated by rotor-stator interaction is designed to be cut-off by the blade and vane count. The first harmonic of the blade rate tone occurs at twice the blade passing frequency (2×BPF), which at approach speed is 2×5425 RPM / 60 s/min × 18 blades = 3255 Hz, as seen in Figure 16. The amplitude of the tone was calculated by integrating under several bins in the spectra where the tone energy is distributed. Details about this process was discussed by Svetgoff et al. [25]. The resulting directivity for 2×BPF is given in Figure 19 for approach fan speed and Figure 20 for takeoff fan speed. For clarity, only Mach 0.1 and 0.2 are shown. In both cases, increasing the tunnel speed decreased the aft radiated peak tone level. For 5425 RPMc the directivity pattern is shifted upstream despite the correction for emission angle. Otherwise, general trends are difficult to draw. The higher frequency tones have inherently more complicated directivity and a thorough discussion is beyond the scope of the present paper. The data set is readily available in [7].

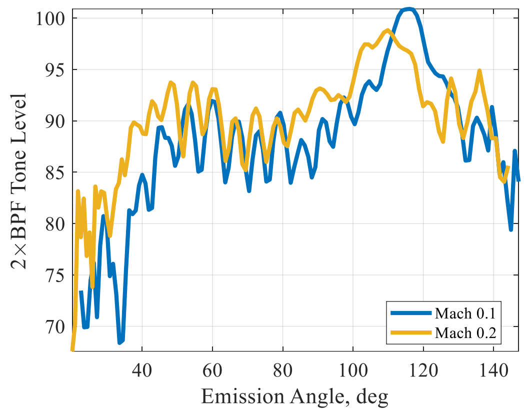

Figure 19 - 2×BPF tone level at 5425 RPMc

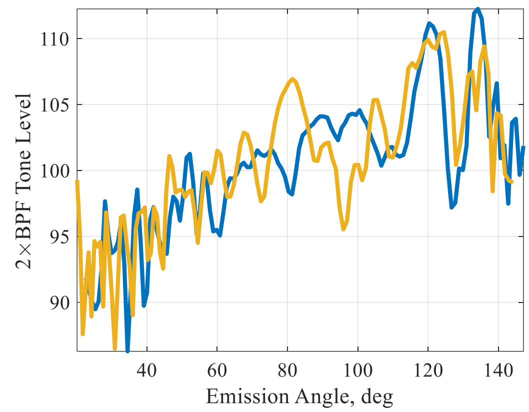

Figure 20 - 2×BPF tone level at 8750 RPMc

B. New Testing Capability

The lower background levels of the facility enable measurement conditions that previously had bad signal to noise levels. For example, the data in Figure 21 shows the same model and configuration used in the commissioning test but from a 2006 tunnel entry. The tunnel speed was limited to Mach 0.1 for an acceptable signal-to-noise ratio. The tunnel background noise, described in Figure 2, was repeated. This data can now be acquired with good signal-to-noise ratio at Mach 0.2, as shown in Figure 22. Measurements of the broadband noise from an open rotor at low shaft speed should be possible, although this has not been demonstrated yet. Testing of small electric propulsors is also enabled.

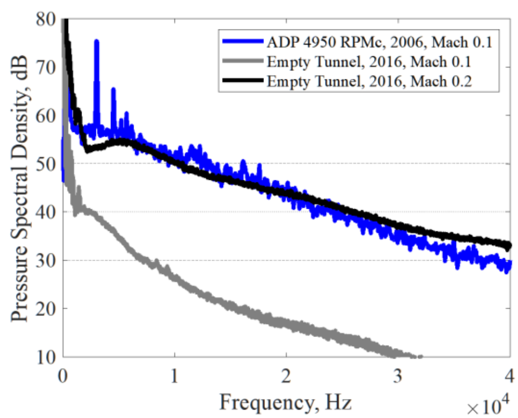

Figure 21 Legacy ADP fan data acquired at Mach 0.1

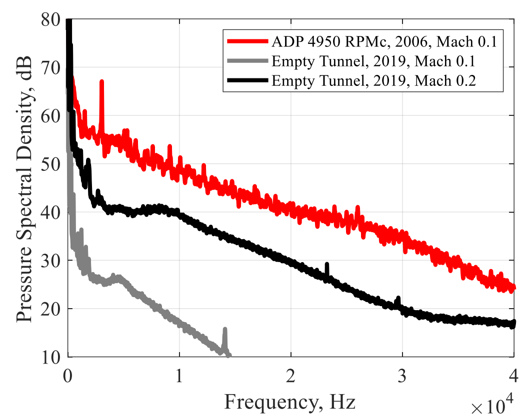

Figure 22 New ADP fan data acquired at Mach 0.2

C. Historical Testing at Mach 0.1

Past tunnel testing has been conducted at Mach 0.1 to limit background noise. Entire test campaigns would be conducted at Mach 0.1 only. The data set from the commissioning test can be used to help determine what affect this limitation has had and the implication for legacy fan data. This effort has not been started so far.

D. Forward Flight Effect for System Noise

The impact of forward flight on fan noise has been the subject of considerable investigation. Analytical work has been done by many authors including Amiet [26] and Rice [27], but the problem is sufficiently challenging that significant simplifications are required for the mathematics to be tractable. Extensive experimental work spanning test stands, wind tunnels and flight tests [28] [29] have been conducted to address the topic and guide the acoustic community to obtain a relatively simple correction. The commonly used convective amplification correction is nicely described in section 3.1.3 of the report by Lieber and Elkins [30] and their notation is reproduced here. Given the mean-square sound pressure $p_s^2(\theta_e)$ measured with a zero forward flight, such as an engine on a test stand, the mean-square sound pressure in forward flight $p_f^2(\theta_e)$ is calculated by,

$$p_f^2(\theta_e) = \frac{p_s^2(\theta_e)}{(1-M\cos\theta_e)^{\alpha}},$$

where θ_e is the emission angle between the source and observer measured from upstream, M is the forward flight Mach number and α is the convective amplification constant. A value of α = 4 is described in [30] as correct for ducted fans while α = 2 is used for propellers, at least by Berton [31]. In this way, an enormous amount of theoretical and experimental work on a complicated engineering and mathematical system is reduced to a simple correction.

The data set described here could be used to investigate this further. To calculate the amplification in decibels between two different tunnel Mach numbers M_A and M_B,

$$\Delta\text{SPL} = \alpha\, 10\log_{10}\left(\frac{(1-M_A\cos\theta_e)}{(1-M_B\cos\theta_e)}\right).$$

This is compared in Figure 23 against the measured result for the OASPL broadband noise change between Mach 0.1 and Mach 0.2 previously plotted in Figure 17 and Figure 18. The data set from the commissioning test could be used to investigate the forward flight effect and associated impact on fan system noise modeling.

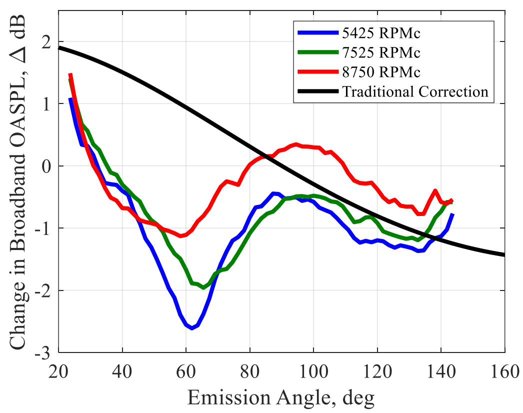

Figure 23 Effect of tunnel speed on broadband level

VI.Conclusion

The NASA GRC 9×15 LSWT acoustic upgrade was successfully completed and a commissioning test has been conducted that demonstrates the safe operation and new capabilities for propulsor testing. The ADP fan model is reasonably representative of the noise levels of quiet fans anticipated in the foreseeable future and demonstrates that even low power settings can be tested at high tunnel speeds with good signal-to-noise ratio. Future plans for the data set include advanced signal processing using a recently developed software package for scanning microphones [32]. The data from the present test along with the fan geometry is published in a NASA Technical Memorandum test report by the present authors and it is hoped that it will be of use to the aeroacoustics community [7].

Acknowledgments

This work was supported by the NASA Advanced Air Transport Technology project of the Advanced Air Vehicles Program. Thanks also to the 8×/9× wind tunnel complex staff who assembled the model and ran the test. Thanks especially to Linda Bartos who was lead test engineer for this tunnel entry.

VII.References

[1] D. B. Stephens, D. E. Van Zante and D. E. Stark, "Overview of the Acoustic Improvement Program for the 9-by 15-Foot Low Speed Wind Tunnel (AIAA 2021-2969)," in *AIAA AVIATION 2021 FORUM*, Virtual, August 2-6, 2021.

[2] D. Rinehart and A. Johnson, "Full Aero-Thermal Characterization of Acoustic Improvements to the 9- by- 15 Foot Low Speed Wind Tunnel (AIAA 2021-2971)," in *AIAA AVIATION 2021 FORUM*, Virtual, August 2-6, 2021.

[3] D. B. Stephens, "Acoustic Improvements to the 9- by 15-Foot Low Speed Wind Tunnel (AIAA 2021-2972)," in *AIAA AVIATION 2021 FORUM*, Virtual, August 2-6, 2021.

[4] P. Agarwal, C. C. J. Yen, M. Karanikolov, S. Best, T. Nagle and E. Duell, "Computational Verification Analysis of 9- by 15- Foot Low Speed Wind Tunnel Acoustic Upgrade Design (AIAA 2021-2970)," in *AIAA AVIATION 2021 FORUM*, Virtual, August 2-6, 2021.

[5] D. B. Stephens, M. J. Krupar, C. J. Miller and S. J. Sedensky, "9- by 15-Foot Low-Speed Wind Tunnel Acoustic Upgrade Part 1: Supporting Studies," NASA/TM-20210024786/Part1, July 2022.

[6] D. B. Stephens, M. J. Krupar, C. J. Miller and S. J. Sedensky, "9- by 15-Foot Low-Speed Wind Tunnel Acoustic Upgrade Part 2: Improvement Comparison," NASA Glenn Research Center , Cleveland, Ohio, United States, July 2022.

[7] D. B. Stephens, D. M. Elliott and J. A. Gazzaniga, "9- by 15-Foot Low-Speed Wind Tunnel Commissioning Test Using the Advanced Ducted Propulsor," NASA, Cleveland, Ohio, USA, 2025.

[8] P. E. Rentz, "Hardwall Acoustical Characteristics and Measurement Capabilities of the NASA Lewis 9 x 15 Foot Low Speed Wind Tunnel," NASA Lewis Research Center, Cleveland, Ohio, USA, September 1976.

[9] P. E. Rentz, "Softwall Acoustical Characteristics and Measurement Capabilities of the NASA Lewis 9 x 15 Foot Low Speed Wind Tunnel CR-135025," NASA Lewis Research Center, October 1976.

[10] M. D. Dahl and E. J. Rice, "Measured acoustic properties of variable and low density bulk absorbers (NASA TM-87065)," in *1985 Winter Annual Meeting of the American Society of Mechanical Engineers*, Miami Beach, Florida, USA, 17-21 November 1985.

[11] M. D. Dahl and R. P. Woodward, "Comparison between design and installed acoustic characteristics of NASA Lewis 9- by 15-foot low-speed wind tunnel acoustic treatment," NASA TP-2966, 1990.

[12] M. D. Dahl and R. P. Woodward, "Acoustical evaluation of the NASA Lewis 9 by 15 foot low speed wind tunnel (NASA-TP-3274)," NASA Lewis Research Center, Cleveland, Ohio, USA, November 1992.

[13] R. P. Woodward, J. H. Dittmar, D. G. Hall and B. Kee-Bowling, "Background Noise Levels Measured in the NASA Lewis 9- by 15-Foot Low-Speed Wind Tunnel (NASA TM-106817)," in *33rd Aerospace Sciences Meeting and Exhibit sponsored by the American Institute of Aeronautics and Astronautics*, Reno, Nevada, USA, 9-12 January 1995.

[14] D. B. Stephens, "The Acoustic Environment of the NASA Glenn 9- by 15-Foot Low-Speed Wind Tunnel," in *21st AIAA/CEAS Aeroacoustics Conference*, Dallas, Texas, USA, 22-26 June 2015.

[15] D. B. Stephens, "Data Summary Report for the Open Rotor Propulsion Rig Equipped With F31/A31 Rotor Blades (NASA TM—2014-216676)," NASA Glenn Research Center, Cleveland, Ohio, USA, November 2014.

[16] D. E. Hobbs, R. J. Neubert, E. W. Malmborg, D. H. Philbrick and D. A. Spear, "Low Noise Research Fan Stage Design," NASA-CR-195382, 1995.

[17] R. J. Jeracki, "Comprehensive Report of Fan Performance From Duct Rake Instrumentation on 1.294 Pressure Ratio, 806 ft/sec Tip Speed Turbofan Simulator Models," NASA Glenn Research Center, Cleveland, Ohio, United States, 2006.

[18] J. H. Dittmar, D. M. Elliott and L. A. Bock, "Some Acoustic Results from the Pratt and Whitney Advanced Ducted Propulsor: Fan 1," NASA Glenn Research Center , Cleveland, OH United States, March 1999.

[19] E. Envia, "Acoustic Power Transmission Loss Through a Ducted Fan," in *22nd AIAA/CEAS Aeroacoustics Conference*, Lyon, France, 2016.

[20] C. Balan and G. E. Hoff, "Propulsion Simulator for High Bypass Turbofan Performance Evlauation," in *SAE Aerospace Atlantic Conference & Exposition*, Dayton, Ohio, United States, 1993.

[21] C. S. Allen and P. T. Soderman, "Aeroacoustic Probe Design for Microphone to Reduce Flow-Induced Self-Noise (AIAA 93-4343)," in *15th AIAA Aeroacoustics Conference*, Long Beach, California, USA, 25-27 October 1993.

[22] C. S. Allen, K. Vandra and P. T. Soderman, "Microphone Corrections for Accurate In-Flow Acoustic Measurements at High Frequency," in *First Joint CEAS/AIAA Aeeroacoustics Conference*, Munich, Germany, 12-15 June 1995.

[23] C. A. Brown and D. B. Stephens, "Acoustic Methods Used in the NASA Glenn 9- by 15- Foot Low-Speed Wind Tunnel," NASA TM 2018-218874, June 2018.

[24] D. Sree and D. B. Stephens, "Improved Separation of Tone and Broadband Noise Components from Open Rotor Acoustic Data," *Aerospace,* vol. 3, no. 3, 2016.

[25] A. A. Svetgoff, D. B. Stephens and E. Envia, "Inlet Radiated Noise Predictions for the NASA Source Diagnostic Test Fan Using Physics-Based Simulations," in *28th AIAA/CEAS Aeroacoustics Conference*, Southhampton, Great Britan, June 2022.

[26] R. K. Amiet, "Correction of fan noise for effects of forward flight," *Journal of Sound and Vibration,* vol. 89, no. 2, pp. 243-259, 1983.

[27] E. J. Rice, "Aircraft inlet noise radiation model static, flight and bellmouth effect," in *2nd AIAA and CEAS, Aeroacoustics Conference,* State College, Pennslvania, USA, May 6-8, 1996.

[28] C. E. Feiler and J. E. Merriman, "EFFECTS OF FORWARD VELOCITY AND ACOUSTIC TREATMENT ON INLET FAN NOISE," in *Sixth Aircraft Design Flight Test and Operations Meeting*, Los Angeles, California, USA, August 12-14, 1974.

[29] J. S. Preisser and D. Chestnutt, "Flight effects on fan noise with static and wind-tunnel comparisons," *Journal of aircraft,* vol. 21, no. 7, pp. 453-461, 1984.

[30] L. S. Lieber and D. Elkins, "Small Engine Technology (SET). Task 33: Airframe, Integration, and Community Noise Study NASA/CR-2002-211670," NASA Langley Research Center, October 2002.

[31] J. J. Berton, "Empennage Noise Shielding Benefits for an Open Rotor Transport," in *17th Aeroacoustics Conference* , Portland, Oregon, USA, 5-8 June 2011.

[32] P. N. Shah, D. Hensley, D. Papamoschou and D. Stephens, "WIND TUNNEL CONTINUOUS-SCAN ACOUSTIC ANALYSIS OF DUCTED FAN TONES INTERACTING WITH A SHIELDING WALL," in *ASME Turbo Expo 2025 Turbomachinery Technical Conference and Exposition*, Memphis, Tennessee, USA, 16-20 June 2025.